Supplemental Information for

Extension of the AIOMFAC model by iodine and carbonate species: applications for aerosol acidity and cloud droplet activation

Hang Yin et al.

Correspondence: Andreas Zuend (andreas.zuend@mcgill.ca)

S1 Extra systems of iodide salts with organic compounds

Figure S1 shows some additional systems of liquid–liquid equilibrium (LLE), mean molal activity coefficients of NaI ($\gamma_{\pm}$), vapor–liquid equilibrium (VLE), and solubility (SLE) experimental data and corresponding model calculations for iodide salt + various organic compounds. Figure S1a is a LLE system of water + 2-butanone + KI at 298.15 K. This is an example where AIOMFAC predictions show significant deviations from experimental data. However, we note that the LLE of water + 2-butanone mixed with other salts tend to exhibit a phase diagram more similar to what AIOMFAC predicts here for the KI case; hence, this seems to be a rather special behavior due to the iodide salt. Mean molal activity coefficients of NaI in a ternary system of water + maltose + NaI at 298.15 K are shown in Fig. S1b. To enable a direct comparison between the experimental data and AIOMFAC calculations, the reference solvent of the ion activity coefficients is here defined as the water + maltose solvent mixture instead of pure water (the default AIOMFAC setting). AIOMFAC agrees well with the measurements in the water-rich regime, while over-predicting $\gamma_{\pm}(\mathrm{Na^+}, \mathrm{I^-})$ by around 0.2 units when maltose becomes concentrated. Figure S1c shows a water-free VLE system of methanol + benzene + NaI from 332 to 336 K. AIOMFAC predicts significant salting-out behavior on benzene in contrast to experimental results at the most dilute range. The solubility of 2-hydroxybenzoic acid in the mixture of water + KI at 308 K is shown in Fig. S1d. AIOMFAC agrees well with the experimental results, although the concentration of the organic compound is rather low.

S2 Computations of CCN activation

Tables S1 and S2 list the AIOMFAC predictions of the critical supersaturation values for CCN activation, $\mathrm{SS_{crit}}$, for different particle dry diameters and organic volume fractions in aqueous NaI or $\mathrm{Na_2CO_3}$ particles mixed with suberic acid.

S3 Solving the coupled system of equilibrium equations of the carbonate/bicarbonate/$\mathrm{CO_2}$ system

Among the essential components in the carbonic acid system, the molar amounts of three species out of $\mathrm{HCO_3^-}$, $\mathrm{CO_3^{2-}}$, $\mathrm{CO_{2(aq)}}$, $\mathrm{H^+}$, $\mathrm{OH^-}$, and $\mathrm{H_2O}$ are independent. This brings the number of independent (solver) variables to three; although,

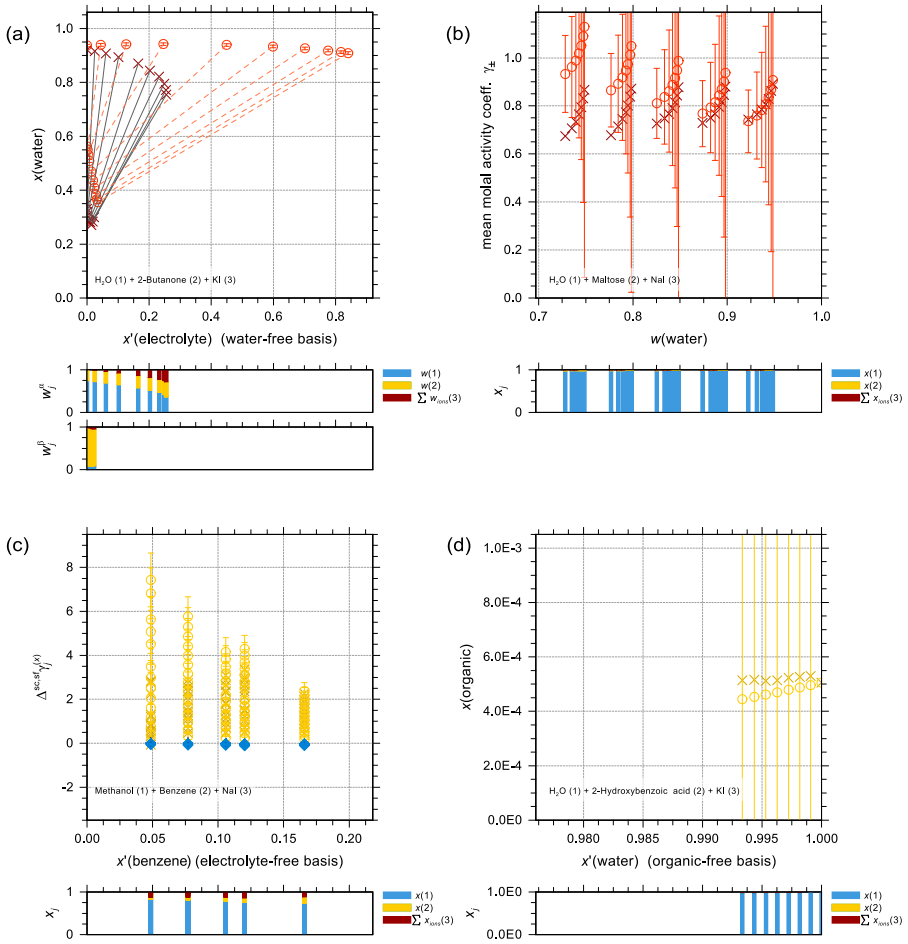

Figure S1. Different types of experimental data (×, +) and AIOMFAC predictions (○, ◇) for organic compounds + iodide salt systems with model sensitivity indicated by error bars. **(a)** LLE of water (1) + 2-butanone (2) + KI (3) at 298 K; experiments by Al-Sahhaf et al. (1999). **(b)** Mean molal activity coefficients of NaI in water (1) + maltose (2) + NaI (3) mixtures at 298 K; experiments by Zhuo et al. (2008). **(c)** VLE of methanol (1) + benzene (2) + NaI (3) at 332–336 K; experiments by Yang et al. (2007). **(d)** SLE of water (1) + 2-hydroxybenzoic acid (2) + KI (3) at 308 K; experiments by Sugunan and Thomas (1995). The composition bar graphs show the mass fractions (in a) or the mole fractions (b, c, d) of the components with respect to dissociated salts.

Table S1. Predictions of the critical supersaturation, SS_{crit} (%), for the CCN activation of mixed water + suberic acid + NaI particles at 293.15 K. The values are listed for distinct particle dry diameters and a selection of organic volume fractions within the dry particles (f_{org}).

Mixture		Dry diameter (nm)											
Solutes	f_{org}	30	35	40	45	50	59	80	100	120	140	160	200
AIOMFAC-EQUIL; with full liquid–liquid phase separation													
NaI		1.064	0.843	0.689	0.577	0.492	0.383	0.242	0.173	0.131	0.104	0.085	0.061
Suberic + NaI	0.27	1.080	0.857	0.701	0.587	0.501	0.390	0.246	0.176	0.134	0.106	0.087	0.062
Suberic + NaI	0.41	1.094	0.868	0.711	0.595	0.508	0.396	0.250	0.179	0.136	0.108	0.088	0.063
Suberic + NaI	0.49	1.104	0.877	0.718	0.601	0.513	0.400	0.253	0.181	0.137	0.109	0.089	0.064
Suberic + NaI	0.53	1.110	0.882	0.722	0.605	0.517	0.403	0.255	0.182	0.138	0.110	0.090	0.064
Suberic + NaI	0.56	1.115	0.886	0.726	0.608	0.519	0.405	0.256	0.183	0.139	0.110	0.090	0.064
Suberic + NaI	0.66	1.137	0.904	0.741	0.621	0.530	0.414	0.262	0.187	0.142	0.113	0.092	0.066
Suberic + NaI	0.78	1.179	0.938	0.769	0.645	0.551	0.430	0.273	0.195	0.148	0.118	0.096	0.069
Suberic + NaI	0.88	1.245	0.991	0.813	0.682	0.583	0.455	0.288	0.206	0.157	0.125	0.102	0.073
AIOMFAC-CLLPS (with org. film); organic phase assumed water-free													
Suberic + NaI	0.27	1.002	0.794	0.649	0.543	0.464	0.361	0.228	0.163	0.124	0.098	0.080	0.057
Suberic + NaI	0.41	0.959	0.760	0.621	0.520	0.444	0.346	0.218	0.156	0.118	0.094	0.077	0.055
Suberic + NaI	0.49	0.931	0.738	0.604	0.505	0.431	0.336	0.212	0.152	0.115	0.091	0.075	0.053
Suberic + NaI	0.53	0.917	0.726	0.594	0.497	0.424	0.331	0.209	0.149	0.113	0.090	0.074	0.053
Suberic + NaI	0.56	0.905	0.717	0.586	0.491	0.419	0.326	0.206	0.147	0.112	0.089	0.073	0.052
Suberic + NaI	0.66	0.863	0.684	0.559	0.468	0.399	0.311	0.197	0.141	0.107	0.085	0.069	0.050
Suberic + NaI	0.78	0.803	0.637	0.521	0.436	0.372	0.290	0.184	0.131	0.100	0.079	0.065	0.046
Suberic + NaI	0.88	0.745	0.591	0.483	0.405	0.346	0.269	0.170	0.122	0.093	0.074	0.060	0.043
AIOMFAC-CLLPS (without org. film); water uptake by organic-rich phase													
Suberic + NaI	0.27	1.056	0.843	0.692	0.582	0.497	0.389	0.246	0.176	0.134	0.106	0.087	0.062
Suberic + NaI	0.41	1.075	0.857	0.704	0.591	0.506	0.395	0.250	0.179	0.136	0.108	0.088	0.063
Suberic + NaI	0.49	1.089	0.868	0.713	0.599	0.512	0.400	0.253	0.181	0.138	0.109	0.089	0.064
Suberic + NaI	0.53	1.097	0.875	0.718	0.603	0.516	0.403	0.255	0.183	0.139	0.110	0.090	0.064
Suberic + NaI	0.56	1.104	0.880	0.723	0.607	0.519	0.405	0.257	0.184	0.140	0.111	0.091	0.065
Suberic + NaI	0.66	1.133	0.903	0.741	0.622	0.532	0.415	0.263	0.188	0.143	0.113	0.093	0.066
Suberic + NaI	0.78	1.188	0.946	0.776	0.651	0.556	0.434	0.275	0.196	0.149	0.118	0.097	0.069
Suberic + NaI	0.88	1.270	1.010	0.827	0.693	0.591	0.461	0.292	0.208	0.158	0.126	0.103	0.073

Table S2. AIOMFAC predictions of critical supersaturation, SS_{crit} (%), for different dry diameters and organic dry volume fractions (f_{org}) of water + suberic acid + Na_2CO_3 particles at 293.15 K.

Mixture		Dry diameter (nm)											
Solutes	f_{org}	30	35	40	45	50	60	80	100	120	140	160	200
AIOMFAC-EQUIL; with full liquid–liquid phase separation													
Na_2CO_3	0.00	0.727	0.573	0.466	0.388	0.330	0.256	0.160	0.113	0.086	0.068	0.055	0.039
Suberic + Na_2CO_3	0.27	0.830	0.655	0.533	0.445	0.378	0.293	0.184	0.130	0.099	0.078	0.063	0.045
Suberic + Na_2CO_3	0.49	0.955	0.755	0.616	0.514	0.438	0.340	0.213	0.151	0.115	0.091	0.074	0.053
Suberic + Na_2CO_3	0.66	1.101	0.873	0.713	0.597	0.508	0.395	0.249	0.177	0.134	0.106	0.086	0.062
Suberic + Na_2CO_3	0.78	1.258	1.000	0.818	0.686	0.585	0.456	0.288	0.205	0.155	0.123	0.100	0.072
Suberic + Na_2CO_3	0.88	1.466	1.168	0.958	0.804	0.687	0.536	0.339	0.243	0.184	0.146	0.119	0.085
AIOMFAC-CLLPS (with org. film); organic phase assumed water free													
Suberic + Na_2CO_3	0.27	0.768	0.606	0.493	0.412	0.350	0.272	0.170	0.121	0.092	0.072	0.059	0.042
Suberic + Na_2CO_3	0.49	0.807	0.637	0.520	0.434	0.370	0.287	0.180	0.128	0.097	0.077	0.063	0.045
Suberic + Na_2CO_3	0.66	0.843	0.666	0.544	0.455	0.387	0.301	0.190	0.135	0.103	0.081	0.066	0.047
Suberic + Na_2CO_3	0.78	0.872	0.690	0.564	0.472	0.402	0.313	0.198	0.141	0.107	0.085	0.069	0.050
Suberic + Na_2CO_3	0.88	0.900	0.713	0.583	0.488	0.416	0.324	0.205	0.146	0.111	0.088	0.072	0.052
AIOMFAC-CLLPS (without org. film); water uptake by organic-rich phase													
Suberic + Na_2CO_3	0.27	0.813	0.645	0.527	0.440	0.375	0.291	0.183	0.130	0.098	0.078	0.063	0.045
Suberic + Na_2CO_3	0.49	0.944	0.749	0.612	0.512	0.436	0.339	0.213	0.151	0.115	0.091	0.074	0.053
Suberic + Na_2CO_3	0.66	1.104	0.876	0.716	0.599	0.511	0.397	0.250	0.178	0.134	0.106	0.087	0.062
Suberic + Na_2CO_3	0.78	1.284	1.019	0.833	0.697	0.594	0.462	0.291	0.207	0.157	0.124	0.101	0.072
Suberic + Na_2CO_3	0.88	1.530	1.215	0.992	0.829	0.707	0.549	0.346	0.246	0.187	0.148	0.121	0.086

for numerical reasons discussed further below, it can be advantageous to use a larger number of "solver variables" (solving a coupled system of equations including molar balance equations). At the start of the equilibrium calculation for a given mixture in terms of input component mass fractions (and pertaining ion molalities), the solution is assumed (an arbitrary choice) to contain 1 kg of solvent mass (i.e., water or water + organics solvent mixture) to generate the initial molar amounts of all ions and neutral species. Since the amount of water in the system is subject to change due to auto-dissociation (React. R3) and/or bicarbonate dissociation (React. R1), use of molar species amounts (n_i) in molar balances is favored over that of molalities (m_i), because molalities would be affected by variations in the effective solvent mass. Converting from the intensive mass fraction quantities to extensive molar amounts is only done in the process of solving for the equilibrium solution speciation, which can then be converted back to mass fraction and molality amounts. If OH^- is not present in the form of an input ion (as part of an input electrolyte component) in the carbonic acid system, its maximum molar amount is directly derived from the fraction (r; Eq. 16) of the initial water amount that is considered as available for auto-dissociation. To fulfill the molar balance constraints of the system, Eqs. (14) and (15), detailing the maximum available molar amounts of each species, have to be fulfilled. As a further molar constraint, the maximum possible amount of $CO_{2(aq)}$ (for a closed-system case) is determined

based on Eqs. (14) and (15) as

$$n_{\mathrm{CO_2}}^{\max} = \min\left[0.5 \cdot n_{\mathrm{H^+}}^{\max},\ n_{\mathrm{CO_3^{2-}}}^{\max}\right]. \tag{S1}$$

Two different approaches for solving the coupled system of equations numerically were implemented. The basis for both are the equilibrium relationships (Eqs. 8–11) and the molar balance constraints. Associated numerical advantages and drawbacks were evaluated below. The first approach labeled "ratio approach" is discussed in the following.

S3.1 Ratio approach

The independent species amounts chosen for solving the coupled equations are the molar amounts of $\mathrm{HCO_3^-}$, $\mathrm{CO_3^{2-}}$, and $\mathrm{OH^-}$. While other choices could be made, e.g., using $\mathrm{H^+}$ as an independent species/variable instead of $\mathrm{HCO_3^-}$, such a choice would complicate the expressions since $\mathrm{H^+}$ could stem from many other mixture components, including from bisulfate and sulfuric acid. The remaining species are determined by ensuring that the molar balances (Eqs. 14 and 15) are fulfilled. Since the differences between the absolute molar amounts of the different species can span several orders of magnitude, the actual solver variables are expressed using ratios involving the maximum possible amounts and ratio adjustment for reasons of numerical precision. For example, the solver variable $r_{\mathrm{OH^-}}^{\mathrm{Solv}}$ is computed using

$$r_{\mathrm{OH^-}}^{\mathrm{Solv}} = \frac{r_{\mathrm{OH^-}} - r_{\mathrm{OH^-}}^{\min}}{r_{\mathrm{OH^-}}^{\max} - r_{\mathrm{OH^-}}^{\min}}. \tag{S2}$$

For r_i^{Solv} to be physically meaningful, the minimum and maximum adjustment values are defined based on the $[0, 1]$ interval limit as

$$r_i^{\text{Solv, min}} = N_{\text{tiny}}, \tag{S3}$$

$$r_i^{\text{Solv, max}} = 1.0 - N_{\text{tiny}}. \tag{S4}$$

Here, N_{tiny} is set as $3.0 \cdot \epsilon$ where ϵ is the machine precision (a value of about 10^{-15} in our program).

S3.1.1 The limits of $r_{\mathrm{HCO_3^-}}$

Being the principle independent species in our setup, $n_{\mathrm{HCO_3^-}}$ is allowed to vary between a very small amount and nearly its maximum amount ($n_{\mathrm{HCO_3^-}}^{\max}$) which leaves the limits of $r_{\mathrm{HCO_3^-}}$ as

$$r_{\mathrm{HCO_3^-}}^{\min} = N_{\text{tiny}}, \tag{S5}$$

$$r_{\mathrm{HCO_3^-}}^{\max} = 1.0 - N_{\text{tiny}}. \tag{S6}$$

As a result, $r_{\mathrm{HCO_3^-}}^{\mathrm{Solv}}$ is bounded by the same limits as Eqs. (S5)–(S6).

S3.1.2 The limits of $r_{\mathrm{CO_3^{2-}}}$

The minimum limits of $r_{\mathrm{CO_3^{2-}}}$ and $r_{\mathrm{OH^-}}$ are determined from the relationship (Eqs. 14–15) and assumptions expressed by the molar balance equations due to a certain value of $n_{\mathrm{HCO_3^-}}$ determined by a given $r_{\mathrm{HCO_3^-}}$ value. That is, there is no independent choice for their limits when the goal is to ensure all molar balance constraints remain exactly fulfilled for any possible choice of the set of solver variables during the iterative solving of the system of equations. Maintaining such mathematical and chemical consistency is critical in avoiding intermediate mixture composition involving negative molar amounts of certain species. In the case of $\mathrm{CO_3^{2-}}$, by assuming $n_{\mathrm{CO_{2(aq)}}}$ is at its upper limit, $n^{\mathrm{max}}_{\mathrm{CO_{2(aq)}}}$, the first limit is given by

$$r^{\mathrm{min1}}_{\mathrm{CO_3^{2-}}} = \frac{n^{\mathrm{max}}_{\mathrm{CO_3^{2-}}} - n_{\mathrm{HCO_3^-}} - n^{\mathrm{max}}_{\mathrm{CO_2}}}{n^{\mathrm{max}}_{\mathrm{CO_3^{2-}}} - n_{\mathrm{HCO_3^-}}}. \tag{S7}$$

Following the same logic, the second limit is determined by leaving potential room for $\mathrm{H^+}$ based on Eq. 15,

$$r^{\mathrm{min2}}_{\mathrm{CO_3^{2-}}} = \frac{n^{\mathrm{max}}_{\mathrm{CO_3^{2-}}} - 0.5 \cdot n_{\mathrm{HCO_3^-}} - 0.5 \cdot n^{\mathrm{max}}_{\mathrm{H^+}} \cdot (1-\epsilon)}{n^{\mathrm{max}}_{\mathrm{CO_3^{2-}}} - n_{\mathrm{HCO_3^-}}}. \tag{S8}$$

Thus, the internal minimum limit of $r_{\mathrm{CO_3^{2-}}}$ should be

$$r^{\mathrm{min}}_{\mathrm{CO_3^{2-}}} = \max\left[r^{\mathrm{min1}}_{\mathrm{CO_3^{2-}}},\ r^{\mathrm{min2}}_{\mathrm{CO_3^{2-}}},\ N_{\mathrm{tiny}}\right]. \tag{S9}$$

To avoid potential numerical issues, $r^{\mathrm{min}}_{\mathrm{CO_3^{2-}}}$ is further constrained to ensure it is less than $1.0 - N_{\mathrm{tiny}}$.

S3.1.3 The limits of $r_{\mathrm{OH^-}}$

As in the case of $\mathrm{OH^-}$, because $n_{\mathrm{H^+}}$ has to be a positive number, based on Eq. (15), $n_{\mathrm{H^+}}$ is computed as

$$n_{\mathrm{H^+}} = n^{\mathrm{max}}_{\mathrm{H^+}} - n^{\mathrm{max}}_{\mathrm{OH^-}} - n_{\mathrm{HCO_3^-}} - 2n_{\mathrm{CO_{2(aq)}}} + n_{\mathrm{OH^-}}. \tag{S10}$$

As some of the $\mathrm{H^+}$ may be consumed by the formation of $\mathrm{HCO_3^-}$ or $\mathrm{CO_{2(aq)}}$, according to Eq. (S10) an equivalent amount of $\mathrm{OH^-}$ is formed in the same process putting a minimum constraint on $n_{\mathrm{OH^-}}$:

$$n^{\mathrm{min}}_{\mathrm{OH^-}} = n^{\mathrm{min}}_{\mathrm{H^+}} - n^{\mathrm{max}}_{\mathrm{H^+}} + n^{\mathrm{max}}_{\mathrm{OH^-}} + n_{\mathrm{HCO_3^-}} + 2n_{\mathrm{CO_{2(aq)}}}. \tag{S11}$$

If $n^{\mathrm{min}}_{\mathrm{H^+}} = 0$, the minimum limit of $\mathrm{OH^-}$ is

$$n^{\mathrm{min}}_{\mathrm{OH^-}} = \max\left[N_{\mathrm{tiny}}, n^{\mathrm{max}}_{\mathrm{OH^-}} - n^{\mathrm{max}}_{\mathrm{H^+}} + n_{\mathrm{HCO_3^-}} + 2n_{\mathrm{CO_{2(aq)}}}\right]. \tag{S12}$$

As a result,

$$r^{\text{min}}_{\text{OH}^-} = \max\left[N_{\text{tiny}}, \frac{n^{\text{min}}_{\text{OH}^-}}{n^{\text{max}}_{\text{OH}^-}}\right]. \tag{S13}$$

The three equilibria denoted by Eqs. (8)–(10) are then solved by iteratively adjusting the r_i^{Solv} values until the right-hand side expressions computed by the derived molar amounts, molalities, and associated activities or activity coefficients of all species in the solution are within a desired numerical tolerance range with the literature values given in Table 4. Here, Powell's hybrid method is used to solve the three coupled equations in three unknowns (Moré et al., 1980, 1984). Powell's hybrid method is an efficient solver for non-linear equations, yet does not allow for box-constraints to be set on the variables; hence, the allowed limits on the r_i^{Solv} variables "proposed" by the solver (Eqs. S3–S4) need to be checked and, if necessary, corrected within our subroutines to maintain feasible values at all times.

Overall, this method is very efficient when all molar species amounts under final equilibrium conditions are well within machine precision (using double-precision floating point numbers), which is usually the case in the dilute to moderately concentrated aqueous solution regime (see Fig. S2a). However, in applications involving more extreme conditions (low water content, very high or very low acidity), some of the species amounts may turn out to be extremely small during the computation (e.g., on the order of 10^{-15} or even smaller) compared to other molar amounts (on the order of 10^{0}). Since this ratio-based approach requires that $n_{\text{CO}_{2(\text{aq})}}$ and n_{H^+} are determined from the molar balance Eqs. (14) and (15), the subtraction of tiny values from larger numbers can lead to a substantial loss of numerical precision (cancellation error and/or round-off error), which will then often result in numerical issues (even when "safe" numerical summation functions are used, see the example shown in Fig. S2b). Hence, to provide a reliable computation over a wide range of acidities and ionic strengths, an alternative approach was implemented, which is discussed in the following.

S3.2 Log-transformed constrained amount approach

Inspired by the constrained nonlinear solver developed by Schittkowski (2006), the problem is re-approached as a constrained optimization problem in which the number of "solver" variables is increased to five. In this approach, the molar amounts of HCO_3^-, CO_3^{2-}, $\text{CO}_{2(\text{aq})}$, H^+, and OH^- were all set as variables to be determined via solver-suggested values. To better account for possible tiny molar amounts of either OH^- or H^+ under highly acidic or basic conditions, we first apply a logarithm transformation, such that the actual solver variables denote the vector of natural logarithms of the molar amounts (instead of absolute molar amounts). As with the ratio approach, Powell's hybrid method was still chosen as the algorithm to solve the nonlinear system of equations. During each iteration, all species amounts are constrained to be between a tiny positive number (N_{tiny1}) and their near maximum molar amounts for higher solving efficiency. For example, in the case of H^+, its minimum

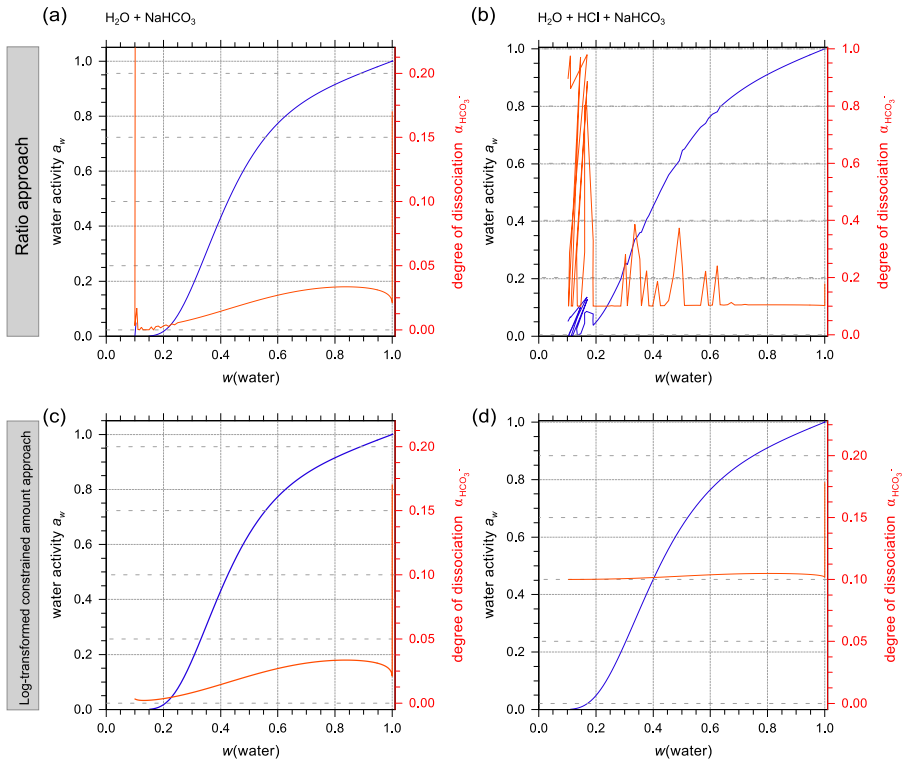

Figure S2. Comparison of AIOMFAC calculations using two different approaches for closed carbonate/bicarbonate/CO_2 systems. Predictions are based on ratio approach (top) and log-transformed constrained amount approach (bottom). **(a, c)** Aqueous $NaHCO_3$ solutions at 298 K. **(b, d)** Aqueous $HCl + NaHCO_3$ solutions mixed 1:10 by moles at 298 K.

and maximum limits are expressed as

$$\ln\left[n_{H^+}^{\min}\right] = \ln[N_{\text{tiny1}}], \tag{S14}$$

$$\ln\left[n_{H^+}^{\max}\right] = \ln\left[(1.0 - N_{\text{tiny2}}) \cdot n_{H^+}^{\max}\right]. \tag{S15}$$

Here, the tiny number is modified to be more meaningful in the context of log-transformation with

$$N_{\text{tiny1}} = 10^{-6} \cdot \epsilon, \tag{S16}$$

$$N_{\text{tiny2}} = 5.0 \cdot \epsilon. \tag{S17}$$

In addition to the three equilibrium equations (Eqs. 8–10), two additional equations, the molar balances (Eqs. 14 and 15) have to be fulfilled at the same time. Hence, this constitutes a problem of solving five coupled nonlinear equations in five unknowns.

Despite having more solver variables compared to the ratio approach, this method achieves the same or even higher level of efficiency and better reliability (see Fig. S2c,d). This may be the result of not imposing the molar balance constraints

to be fulfilled at each iteration step, which gives the solver more freedom to explore the solution space, including solving the problem via an iterative path that involves temporary violations of some molar balances. In addition, in the presence of additional partial dissociation equilibria, like that of bisulfate/sulfate, this method allows for an easier addition of another variable (i.e., $\ln[n_{\mathrm{HSO_4^-}}]$) and pertaining equilibrium expressions to be solved simultaneously.

S3.3 Special conditions

Under extremely acidic or basic aqueous solution conditions, the solver is unable to solve the equilibria to a satisfactory tolerance level. This is because of the fact that within the procedure computing the mixture composition and via AIOMFAC activity coefficients, the solver-suggested values need to be transformed via the exponential function into actual molar amounts. Some of those molar amounts or related mass fractions may be smaller than the machine precision value, causing AIOMFAC to return discontinuous numbers under conditions of small variations in the solver variables (see results in Fig. S3b). As a means to avoid issues under such circumstances, an affected ion's molality is instead determined via a reverse calculation using the other ion molalities, activity coefficients, and the known equilibrium constant value. This allows the problem to be solved under such extreme conditions and results in physically reasonable estimations of pH that meet all equilibria and molar balance constraints (see results in Fig. S3a).

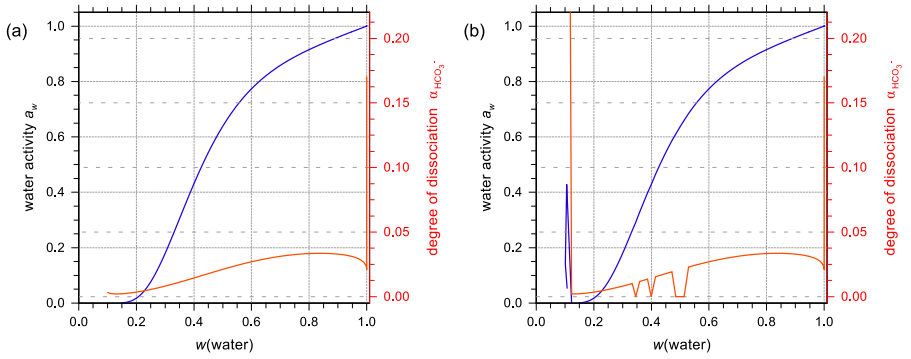

Figure S3. AIOMFAC predictions of water activity and $\mathrm{HCO_3^-}$ degree of dissociation in aqueous $\mathrm{NaHCO_3}$ solutions with the special condition treatment switched on **(a)** and off **(b)** (closed-system).

The above description solves the liquid-phase equilibria in a closed system, while in an open system, Eq. 11 has to be solved alongside as well. The solving principles of an open-system scenario are mostly the same as those of a closed system, except for the constraints for $n^{\mathrm{max}}_{\mathrm{H^+}}$ and $n^{\mathrm{max}}_{\mathrm{CO_3^{2-}}}$ being defined by

$$n^{\mathrm{max}}_{\mathrm{CO_3^{2-}}} = n_{\mathrm{CO_{2(aq)}}} + n_{\mathrm{CO_{2(g)}}} + n_{\mathrm{CO_3^{2-}}} + n_{\mathrm{HCO_3^-}}, \tag{S18}$$

$$n^{\mathrm{max}}_{\mathrm{H^+}} = n_{\mathrm{H^+}} + n_{\mathrm{HCO_3^-}} + 2n_{\mathrm{CO_{2(aq)}}} + 2n_{\mathrm{CO_{2(g)}}} + n^{\mathrm{max}}_{\mathrm{OH^-}} - n_{\mathrm{OH^-}}. \tag{S19}$$

S4 Description of our water activity measurements

Water activity measurements were carried out at McGill University and ETH Zurich to validate existing experimental data or to provide additional measurement data for systems where data available from the scientific literature is scarce. Tables S3–S7 show the bulk water activity data of binary or ternary inorganic solutions measured at McGill University. An AquaLab water activity meter (Model 4TE, METER Group, USA) has been used for bulk measurements based on the dew point method at room temperature ($\sim$ 293.15 K) with a specified precision of ± 0.003 a_w units. The instrument was calibrated using 8.57 M LiCl solutions of well-known $a_w = 0.496$ ($\sim$ 293 K) and deionized water ($a_w = 1.000$) prior to each series of measurements. Inorganic electrolyte samples with purities ≥ 99 % were obtained from the following companies: $\mathrm{HIO_3}$: Sigma-Aldrich, NaBr: BDH Chemicals, KBr: Sigma-Aldrich, $\mathrm{KIO_3}$: Fisher, and $\mathrm{NaIO_3}$: Alfa Aesar. Solutions were prepared by mass fraction of the listed electrolyte components (without further purification) with deionized water. The reported water activity at each composition is the average of three consecutive measurements.

For the measurements done at ETH Zurich, NaI and the relevant organic compounds were purchased from Sigma-Aldrich with 99 % purity. Tables S8–S11 show the bulk water activity data in ternary water + organic compound + NaI mixtures at 298.15 K. An AquaLab water activity meter (Model 3TE, Decagon Devices, USA) with an accuracy of ± 0.003 a_w units has been used for these measurements at 298.15 K. Prior to the measurements, the instrument was calibrated regularly with saturated NaCl solutions ($a_w = 0.753$ at 298.15 K). Samples were always prepared freshly before measurements. Stock solutions were made separately for each chemical species (without further purification) using ultrapure water (resistivity $\geq$18 $\mathrm{M\Omega\,cm}$, MilliQ). The desired concentrations were achieved by mixing and diluting different stock solutions with the reported water activity as the medium of three consecutive measurements. Tables S12–S14 show the EDB water activity data of ternary solutions at various temperatures with the detailed experimental setup discussed elsewhere (Marcolli and Krieger, 2006; Zardini et al., 2008; Steimer et al., 2015). Briefly, we levitated a charged droplet of known dry mass composition in the EDB at a fixed temperature and slightly reduced total pressure ($8.0 \cdot 10^4$ Pa) in a nitrogen gas. RH was varied by changing the ratio of dry to humidified gas flows using mass flow controllers, typically the total flow rate was 20 sccm. Relative humidity was measured by a capacitive RH probe with an integrated temperature sensor (U.P.S.I., France, model G-TUS.13R) mounted in the upper-end cap of the EDB in close proximity to the levitated particle. The probe was calibrated by levitating single particles of various salts and observing the RH at which they deliquesce. The composition of the particle was determined as described in detail by Steimer et al. (2015) using Mie resonance spectroscopy in combination with mass data from the voltage compensating the gravitational force. The uncertainty of these data is ± 1.5 % in water activity (because of the hysteresis of the capacitance sensor) and estimated to be better than $\sim$ 0.05 in the mass fraction of solute.

Table S3. Bulk water activity measurements of the system water (1) + $NaIO_3$ (2) at $T = 293.15$ K. Concentrations are given in mass fractions of $NaIO_3$.

$w(NaIO_3)$	a_w
0.0195	0.997
0.0442	0.994
0.0626	0.992
0.0849	0.990

The accuracy of the water activity measurements is specified as ± 0.003 a_w. The uncertainty of the mass fraction is estimated as ± 0.0005.

Table S4. Bulk water activity measurements of the system water (1) + KIO_3 (2) at $T = 293.15$ K. Concentrations are given in mass fractions of KIO_3.

$w(KIO_3)$	a_w
0.0213	0.999
0.0413	0.996
0.0592	0.993
0.0798	0.991

The accuracy of the water activity measurements is specified as ± 0.003 a_w. The uncertainty of the mass fraction is estimated as ± 0.0005.

Table S5. Bulk water activity measurements of the system water (1) + HIO_3 (2) at $T = 293.15$ K. Concentrations are given in mass fractions of HIO_3.

$w(HIO_3)$	a_w
0.0459	0.994
0.0627	0.993
0.1124	0.988
0.1144	0.990
0.1561	0.985
0.1753	0.983
0.2342	0.976
0.2634	0.974
0.3028	0.969
0.3755	0.963
0.4204	0.958
0.4982	0.945
0.6020	0.908
0.6492	0.886

The accuracy of the water activity measurements is specified as ± 0.003 a_w. The uncertainty of the mass fraction is estimated as ± 0.0005.

Table S6. Bulk water activity measurements of the system water (1) + NaBr (2) + $NaIO_3$ (2) at $T = 293.15$ K. Concentrations are given in mass fractions of the salts.

w(NaBr)	$w(NaIO_3)$	a_w
0.0412	0.0074	0.987
0.0835	0.0149	0.971
0.1215	0.0217	0.953
0.1570	0.0281	0.934

The accuracy of the water activity measurements is specified as ± 0.003 a_w. The uncertainty of the mass fraction is estimated as ± 0.0005.

Table S7. Bulk water activity measurements of the system water (1) + KBr (2) + KIO_3 (2) at $T = 293.15$ K. Concentrations are given in mass fractions of the salts.

w(KBr)	$w(KIO_3)$	a_w
0.0682	0.0069	0.985
0.1301	0.0131	0.960
0.1745	0.0176	0.941
0.2415	0.0243	0.909

The accuracy of the water activity measurements is specified as ± 0.003 a_w. The uncertainty of the mass fraction is estimated as ± 0.0005.

Table S8. Bulk water activity measurements of the system water (1) + malonic acid (2) + NaI (3) at $T = 298.15$ K. The organic to inorganic dry mass ratios (OIR) are $1:2$, $2:1$, and ratios in between those. Concentrations are given in mass fractions of malonic acid and NaI.

w(malonic acid)	w(NaI)	a_w
0.3000	0.3000	0.655
0.2000	0.2000	0.859
0.1500	0.1500	0.903
0.1000	0.1000	0.944
0.0750	0.0750	0.958
0.2366	0.3217	0.674
0.1577	0.2145	0.860
0.1183	0.1609	0.911
0.0789	0.1072	0.948
0.0591	0.0804	0.962
0.3000	0.2143	0.772
0.2000	0.1429	0.893
0.1500	0.1071	0.929
0.1000	0.0714	0.958
0.0750	0.0536	0.967
0.1606	0.3211	0.780
0.1070	0.2141	0.886
0.0803	0.1606	0.928
0.0535	0.1070	0.960
0.0401	0.0803	0.969
0.3000	0.1500	0.836
0.2000	0.1000	0.917
0.1500	0.0750	0.944
0.1000	0.0500	0.967
0.0750	0.0375	0.975

The accuracy of the water activity measurements is specified as ± 0.003 a_w.
The uncertainty of the mass fraction is estimated as ± 0.0005.

Table S9. Bulk water activity measurements of the system water (1) + glutaric acid (2) + NaI (3) at $T = 298.15$ K. OIR is $1:1$. Concentrations are given in mass fractions of glutaric acid and NaI.

w(glutaric acid)	w(NaI)	a_w
0.2727	0.2727	0.768
0.1818	0.1818	0.894
0.1364	0.1364	0.931
0.0909	0.0909	0.958
0.0682	0.0682	0.967

The accuracy of the water activity measurements is specified as ± 0.003 a_w.
The uncertainty of the mass fraction is estimated as ± 0.0005.

Table S10. Bulk water activity measurements of the system water (1) + citric acid (2) + NaI (3) at $T = 298.15$ K. OIR is $1:1$. Concentrations are given in mass fractions of citric acid and NaI.

w(citric acid)	w(NaI)	a_w
0.3214	0.3214	0.627
0.2143	0.2143	0.858
0.1607	0.1607	0.916
0.1071	0.1071	0.953
0.1000	0.1000	0.959
0.0804	0.0804	0.967

The accuracy of the water activity measurements is specified as ± 0.003 a_w.
The uncertainty of the mass fraction is estimated as ± 0.0005.

Table S11. Bulk water activity measurements of the system water (1) + sorbitol (2) + NaI (3) at $T = 298.15$ K. OIR is $1:1$. Concentrations are given in mass fractions of sorbitol and NaI.

w(sorbitol)	w(NaI)	a_w
0.3195	0.3195	0.721
0.2832	0.2832	0.790
0.2555	0.2555	0.832
0.2256	0.2256	0.867
0.1883	0.1883	0.903
0.1156	0.1156	0.953
0.0807	0.0807	0.970

The accuracy of the water activity measurements is specified as ± 0.003 a_w.
The uncertainty of the mass fraction is estimated as ± 0.0005.

Table S12. EDB water activity measurements of the system water (1) + glutaric acid (2) + NaI (3) at $T = 279$ K. OIR is $1:1$. Concentrations are given in mass fractions of glutaric acid and NaI.

w(glutaric acid)	w(NaI)	a_w
0.4096	0.4096	0.468
0.4085	0.4085	0.471
0.4011	0.4011	0.489
0.3988	0.3988	0.491
0.3923	0.3923	0.510
0.3899	0.3899	0.513
0.3851	0.3851	0.529
0.3826	0.3826	0.531
0.3778	0.3778	0.544
0.3729	0.3729	0.557
0.3702	0.3702	0.563
0.3649	0.3649	0.577
0.3621	0.3621	0.582
0.3592	0.3592	0.594
0.3540	0.3540	0.607
0.3482	0.3482	0.616
0.3453	0.3453	0.623
0.3400	0.3400	0.638
0.3370	0.3370	0.641
0.3342	0.3342	0.652
0.3282	0.3282	0.660
0.3250	0.3250	0.670
0.3155	0.3155	0.688
0.3120	0.3120	0.692
0.3051	0.3051	0.709
0.3015	0.3015	0.719
0.2947	0.2947	0.727
0.2910	0.2910	0.732
0.2846	0.2846	0.748
0.2815	0.2815	0.753
0.2745	0.2745	0.760
0.2667	0.2667	0.774
0.2587	0.2587	0.786
0.2551	0.2551	0.792
0.2437	0.2437	0.810
0.2339	0.2339	0.833

The accuracy of the water activity measurements is specified as ± 0.015 a_w.
The uncertainty of the mass fraction is estimated as ± 0.05.

Table S13. EDB water activity measurements of the system water (1) + citric acid (2) + NaI (3) at $T = 288$ K.OIR is $1:1$. Concentrations are given in mass fractions of citric acid and NaI.

w(citric acid)	w(NaI)	a_w
0.2060	0.2060	0.862
0.2251	0.2251	0.845
0.2353	0.2353	0.829
0.2420	0.2420	0.818
0.2469	0.2469	0.808
0.2501	0.2501	0.798
0.2540	0.2540	0.788
0.2593	0.2593	0.779
0.2723	0.2723	0.758
0.2799	0.2799	0.737
0.2858	0.2858	0.721
0.2898	0.2898	0.708
0.2930	0.2930	0.697
0.2950	0.2950	0.692
0.2954	0.2954	0.689
0.2975	0.2975	0.688
0.3072	0.3072	0.669
0.3140	0.3140	0.647
0.3191	0.3191	0.630
0.3234	0.3234	0.614
0.3273	0.3273	0.600
0.3291	0.3291	0.593
0.3372	0.3372	0.577
0.3450	0.3450	0.550
0.3494	0.3494	0.532
0.3526	0.3526	0.522
0.3552	0.3552	0.507
0.3571	0.3571	0.497
0.3624	0.3624	0.485
0.3705	0.3705	0.454
0.3750	0.3750	0.433
0.3780	0.3780	0.421
0.3791	0.3791	0.411
0.3801	0.3801	0.406
0.3813	0.3813	0.403
0.3813	0.3813	0.399
0.3837	0.3837	0.391
0.3910	0.3910	0.364

The accuracy of the water activity measurements is specified as ± 0.015 a_w.
The uncertainty of the mass fraction is estimated as ± 0.05.

Table S14. EDB water activity measurements of the system water (1) + sorbitol (2) + NaI (3) at $T = 288.15$ K. OIR is $1:1$. Concentrations are given in mass fractions of sorbitol and NaI.

w(sorbitol)	w(NaI)	a_w
0.2977	0.2977	0.757
0.3081	0.3081	0.739
0.3331	0.3331	0.697
0.3485	0.3485	0.667
0.3580	0.3580	0.647
0.3789	0.3789	0.597
0.3957	0.3957	0.552
0.4110	0.4110	0.510
0.4253	0.4253	0.463
0.4364	0.4364	0.423

The accuracy of the water activity measurements is specified as ± 0.015 a_w. The uncertainty of the mass fraction is estimated as ± 0.05.

References

Al-Sahhaf, T. A., Kapetanovic, E., and Kadhem, Q.: Salt effects on liquid-liquid equilibria in the partially miscible systems water + 2-butanone and water + ethyl acetate, Fluid Phase Equilib., 157, 271–283, https://doi.org/10.1016/S0378-3812(99)00040-0, 1999.

Marcolli, C. and Krieger, U. K.: Phase changes during hygroscopic cycles of mixed organic/inorganic model systems of tropospheric aerosols, J. Phys. Chem. A, 110, 1881–1893, https://doi.org/10.1021/jp0556759, 2006.

Moré, J. J., Garbow, B. S., and Hillstrom, K. E.: User Guide for MINPACK-1, Argonne National Laboratory Report ANL-80-74, Argonne, Ill., USA, http://www.netlib.org/minpack/, 1980.

Moré, J. J., Sorensen, D. C., Hillstrom, K. E., and Garbow, B. S.: The MINPACK Project, in Sources and Development of Mathematical Software, Prentice-Hall, Inc., Upper Saddle River, NJ, USA, 1984.

Schittkowski, K.: NLPQLP: A fortran implementation of a sequential quadratic programming algorithm with distributed and non-monotone line search–user's guide, Report, Department of Computer Science, University of Bayreuth, 2006.

Steimer, S. S., Krieger, U. K., Te, Y.-F., Lienhard, D. M., Huisman, A. J., Luo, B. P., Ammann, M., and Peter, T.: Electrodynamic balance measurements of thermodynamic, kinetic, and optical aerosol properties inaccessible to bulk methods, Atmos. Meas. Tech., 8, 2397–2408, https://doi.org/10.5194/amt-8-2397-2015, 2015.

Sugunan, S. and Thomas, B.: Salting coefficient of hydroxybenzoic acids, Indian J. Chem., Sect A, 34, 134–136, 1995.

Yang, M., Leng, C., Li, S., and Sun, R.: Study of activity coefficients for sodium iodide in (methanol + benzene) system by (vapour + liquid) equilibrium measurements, J. Chem. Thermodyn., 39, 49–54, https://doi.org/10.1016/j.jct.2006.06.002, 2007.

Zardini, A. A., Sjogren, S., Marcolli, C., Krieger, U. K., Gysel, M., Weingartner, E., Baltensperger, U., and Peter, T.: A combined particle trap/HTDMA hygroscopicity study of mixed inorganic/organic aerosol particles, Atmos. Chem. Phys., 8, 5589–5601, https://doi.org/10.5194/acp-8-5589-2008, 2008.

Zhuo, K., Liu, H., Zhang, H., Liu, Y., and Wang, J.: Activity Coefficients and Volumetric Properties for the NaI + Maltose + Water System at 298.15 K, J. Chem. Eng. Data, 53, 57–62, https://doi.org/10.1021/je700366w, 2008.